Fermi National Accelerator Laboratory

FERMILAB-Pub-98/051-T

$1/N_c$ Corrections to the Hadronic Matrix Elements of Q_6 and Q_8 in $K \to \pi\ \pi$ Decays

T. Hambye et al.

Institut für Physik, Universität Dortmund
D-44221 Dortmund, Germany

W. A. Bardeen

Fermi National Accelerator Laboratory
P.O. Box 500, Batavia, Illinois 60510

June 1998

Submitted to *Nuclear Physics B*

Operated by Universities Research Association Inc. under Contract No. DE-AC02-76CH03000 with the United States Department of Energy

Disclaimer

Distribution

DO–TH 97/28
FERMILAB–Pub–98/051-T

$1/N_c$ Corrections to the Hadronic Matrix Elements of Q_6 and Q_8 in $K \to \pi\pi$ Decays *

T. Hambye, G. O. Köhler, E. A. Paschos, and P. H. Soldan

Institut für Physik, Universität Dortmund, D-44221 Dortmund, Germany

W. A. Bardeen

Fermilab, P.O. Box 500, Batavia, IL 60510

PACS numbers: 13.25. Es, 11.15. Pg, 12.39. Fe

Abstract

We calculate long-distance contributions to the amplitudes $A(K^0 \to 2\pi, I)$ induced by the gluon and the electroweak penguin operators Q_6 and Q_8, respectively. We use the $1/N_c$ expansion within the effective chiral lagrangian for pseudoscalar mesons. In addition, we adopt a modified prescription for the identification of meson momenta in the chiral loop corrections in order to achieve a consistent matching to the short-distance part. Our approach leads to an explicit classification of the loop diagrams into non-factorizable and factorizable, the scale dependence of the latter being absorbed in the low-energy coefficients of the effective theory. Along these lines we calculate the one-loop corrections to the $\mathcal{O}(p^0)$ term in the chiral expansion of both operators. In the numerical results, we obtain moderate corrections to $B_6^{(1/2)}$ and a substantial reduction of $B_8^{(3/2)}$.

*This work was supported in part by the Bundesministerium für Bildung, Wissenschaft, Forschung und Technologie (BMBF), 057D093P(7), Bonn, FRG, and DFG Antrag PA-10-1.

1 Introduction

In this article we study long-distance contributions to the $K \to \pi\pi$ decay amplitudes using the $1/N_c$ expansion (N_c being the number of colors) within the framework of the chiral effective lagrangian for pseudoscalar mesons.

The calculation of chiral loop effects motivated by the $1/N_c$ expansion was introduced in Ref. [1] to investigate the $\Delta I = 1/2$ selection rule. These articles considered loop corrections to the current×current operators Q_1 and Q_2. The gluon penguin operator Q_6 was included at the tree level, consistent with the $1/N_c$ expansion since the short-distance (Wilson) coefficient is subleading in N_c. Following the same lines of thought the authors of Ref. [2] performed a detailed analysis of the ratio ε'/ε, which measures the direct CP violation in $K \to \pi\pi$ decays. They included the matrix elements of Q_6 and Q_8 at the tree level in the $1/N_c$ expansion, arguing that their quadratic dependence on the running mass m_s cancels, in the large-N_c limit, the evolution of the coefficient functions in the absence of chiral loops.

In contrast with the $\Delta I = 1/2$ rule, which is governed by Q_1 and Q_2, ε'/ε is dominated by the density×density operators Q_6 and Q_8. Therefore it is important to investigate the $1/N_c$ corrections to the matrix elements of the last two operators. In particular, it must be examined whether the $1/N_c$ corrections significantly affect the large cancellation between the gluon and the electroweak penguin contributions obtained at the tree level in Ref. [2]. In Ref. [3] the analysis of ε'/ε was extended by incorporating in part chiral loops for the density×density operators, i.e., $1/N_c$ corrections to the matrix elements of Q_6 and Q_8. The final result was an enhancement of $\langle Q_6\rangle_{I=0}$ and a decrease for $\langle Q_8\rangle_{I=2}$, which introduces a smaller cancellation between these two operators. As a consequence, the authors found a large positive value for ε'/ε [4].

In this paper we present a new analysis of the hadronic matrix elements of the gluon and the electroweak penguin operators in which we include, in the isospin limit, the first order corrections in the twofold expansion in powers of external momenta, p, and the ratio $1/N_c$, i.e., we present a complete investigation of the matrix elements up to the orders p^2 and p^0/N_c.[1] One improvement concerns the matching of short- and long-distance contributions to the decay amplitudes, by adopting a modified identification of virtual momenta in the integrals of the chiral loops. To be explicit, we consider the two densities in density×density operators to be connected to each other through the exchange of an effective color singlet boson, and identify its momentum with the loop integration variable.

[1] A comprehensive analysis of chiral loop corrections to the $\mathcal{O}(p^2)$ matrix elements will be presented elsewhere.

The effect of this procedure is to modify the loop integrals, which introduces noticeable effects in the final results. More important it provides an unambiguous matching of the $1/N_c$ expansion in terms of mesons to the QCD expansion in terms of quarks and gluons. The approach followed here leads to an explicit classification of the diagrams into factorizable and non-factorizable. Factorizable loop diagrams refer to the strong sector of the theory and give corrections whose scale dependence is absorbed in the renormalization of the chiral effective lagrangian. The non-factorizable loop diagrams have to be matched to the Wilson coefficients and should cancel scale dependences which arise from the short-distance expansion.

The disentanglement of factorizable and non-factorizable contributions is especially important for the calculation of the $\mathcal{O}(p^0/N_c)$ matrix elements of Q_6: although the $\mathcal{O}(p^0)$ term vanishes for Q_6, the non-factorizable loop corrections to this term remain and have to be matched to the short-distance part of the amplitudes. These $\mathcal{O}(p^0/N_c)$ non-factorizable corrections must be considered at the same level, in the twofold expansion, as the $\mathcal{O}(p^2)$ tree contribution and have not previously been calculated. The same procedure is followed for investigating the matrix elements of Q_8. As a final result, we present the numerical values for the matrix elements $\langle Q_6\rangle_0$ and $\langle Q_8\rangle_2$ to orders p^2 and p^0/N_c.

Another improvement is the enlargement of the lagrangian, that is to say, we use the complete chiral effective lagrangian up to $\mathcal{O}(p^4)$. Finally, we include effects of the singlet η_0, which is necessary for the investigation of isospin breaking terms. The latter generate the matrix element $\langle Q_6\rangle_2$ which is important for ε'/ε [5]. Isospin violating terms will be studied in the future. For consistency, and to introduce the general lines of thought, we include here the η_0 also for the computation of the matrix elements $\langle Q_6\rangle_0$ and $\langle Q_8\rangle_2$ in the isospin limit, where its effect is expected to be small.

This paper includes several improvements which are necessary for a complete calculation to orders p^2 and p^0/N_c, as was defined above. It is still necessary to include these improvements for the isospin violating terms, but this will not affect the results for $\langle Q_6\rangle_0$ and $\langle Q_8\rangle_2$ presented here. Furthermore, we can contemplate still higher order corrections which, at present, are beyond the scope of this analysis.

The paper is organized as follows. In Section 2 we review the general framework of the effective low-energy calculation. In Section 3 we discuss the matching of short- and long-distance contributions to the decay amplitudes. Then, in Section 4 we investigate the factorizable $1/N_c$ corrections to the hadronic matrix elements of Q_6 and Q_8, where we show explicitly that the scale dependence resulting from the chiral loop corrections is absorbed in the renormalization of the bare couplings, the mesonic wave functions and masses. This we do on the particle level, as well as, on the level of the operator evolution for which

we apply the background field method. In Section 5 we calculate the non-factorizable loop corrections to the hadronic matrix elements and the corresponding non-factorizable evolution of the density×density operators. In Section 6 we give the numerical values for the matrix elements and the parameters $B_6^{(1/2)}$ and $B_8^{(3/2)}$. The latter quantify the deviation of the matrix elements from those obtained in the vacuum saturation approximation. Finally, we summarize and compare our results with those of the existing analyses.

2 General Framework

Within the standard model the calculation of the $K \to \pi\pi$ decay amplitudes is based on the effective low-energy hamiltonian for $\Delta S = 1$ transitions [6],

$$\mathcal{H}_{eff}^{\Delta S=1} = \frac{G_F}{\sqrt{2}}\, \xi_u \sum_{i=1}^{8} c_i(\mu) Q_i(\mu) \qquad (\,\mu < m_c\,)\,, \tag{1}$$

$$c_i(\mu) = z_i(\mu) + \tau y_i(\mu)\,, \qquad \tau = -\xi_t/\xi_u\,, \qquad \xi_q = V_{qs}^* V_{qd}\,, \tag{2}$$

where the Wilson coefficient functions $c_i(\mu)$ of the local four-fermion operators $Q_i(\mu)$ are obtained by means of the renormalization group equation. They were computed in an extensive next-to-leading logarithm analysis by two groups [7, 8]. Long-distance contributions to the isospin amplitudes A_I are contained in the hadronic matrix elements of the bosonized operators,

$$\langle Q_i(\mu)\rangle_I \equiv \langle \pi\pi,\, I|Q_i(\mu)|K^0\rangle\,, \tag{3}$$

which are related to the $\pi^+\pi^-$ and $\pi^0\pi^0$ final states through the isospin decomposition

$$\langle Q_i(\mu)\rangle_0 \;=\; \frac{1}{\sqrt{6}}\left(2\langle\pi^+\pi^-|Q_i(\mu)|K^0\rangle + \langle\pi^0\pi^0|Q_i(\mu)|K^0\rangle\right)\,, \tag{4}$$

$$\langle Q_i(\mu)\rangle_2 \;=\; \frac{1}{\sqrt{3}}\left(\langle\pi^+\pi^-|Q_i(\mu)|K^0\rangle - \langle\pi^0\pi^0|Q_i(\mu)|K^0\rangle\right)\,. \tag{5}$$

Direct CP violation in $K \to \pi\pi$ decays is dominated by the gluon and the electroweak penguin operators, i.e., by $\langle Q_6\rangle_0$ and $\langle Q_8\rangle_2$, respectively, where

$$Q_6 = -2\sum_{q=u,d,s} \bar{s}(1+\gamma_5)q\,\bar{q}(1-\gamma_5)d\,, \qquad Q_8 = -3\sum_{q=u,d,s} e_q\,\bar{s}(1+\gamma_5)q\,\bar{q}(1-\gamma_5)d\,, \tag{6}$$

and $e_q = (2/3,\, -1/3,\, -1/3)$. This property follows from the large imaginary parts of their coefficient functions. It is the cancellation between the two penguin contributions which gives rise to a small value of the ratio ε'/ε. Consequently, it is important to investigate

whether the degree of cancellation is affected by corrections to the hadronic matrix elements beyond the vacuum saturation approximation (VSA) [9].

There are several realizations of non-perturbative QCD [1, 10, 11, 12]. A recent development is the calculation of $K \to \pi\pi$ from off-shell $K \to \pi$ amplitudes within chiral perturbation theory [13]. We will perform our analysis using the $1/N_c$ approach. To this end we start from the chiral effective lagrangian for pseudoscalar mesons which involves an expansion in momenta where terms up to $\mathcal{O}(p^4)$ are included [14],

$$\begin{aligned}\mathcal{L}_{eff} &= \frac{f^2}{4}\Big(\langle\partial_\mu U^\dagger \partial^\mu U\rangle + \frac{\alpha}{4N_c}\langle \ln U^\dagger - \ln U\rangle^2 + r\langle \mathcal{M}U^\dagger + U\mathcal{M}^\dagger\rangle\Big) + r^2 H_2\langle \mathcal{M}^\dagger\mathcal{M}\rangle \\ &\quad + rL_5\langle \partial_\mu U^\dagger \partial^\mu U(\mathcal{M}^\dagger U + U^\dagger\mathcal{M})\rangle + rL_8\langle \mathcal{M}^\dagger U\mathcal{M}^\dagger U + \mathcal{M}U^\dagger\mathcal{M}U^\dagger\rangle\,, \end{aligned} \tag{7}$$

with $\langle A\rangle$ denoting the trace of A and $\mathcal{M} = \mathrm{diag}(m_u,\, m_d,\, m_s)$. f and r are free parameters related to the pion decay constant F_π and to the quark condensate, respectively, with $r = -2\langle\bar{q}q\rangle/f^2$. In obtaining Eq. (7) we used the general form of the lagrangian [14] and omitted terms of $\mathcal{O}(p^4)$ which do not contribute to the $K \to \pi\pi$ matrix elements of Q_6 and Q_8 or are subleading in the $1/N_c$ expansion.[2] The fields of the complex matrix U are identified with the pseudoscalar meson nonet defined in a non-linear representation:

$$U = \exp\frac{i}{f}\Pi\,, \qquad \Pi = \pi^a\lambda_a\,, \qquad \langle\lambda_a\lambda_b\rangle = 2\delta_{ab}\,, \tag{8}$$

where, in terms of the physical states,

$$\Pi = \begin{pmatrix} \pi^0 + \frac{1}{\sqrt{3}}a\eta + \sqrt{\frac{2}{3}}b\eta' & \sqrt{2}\pi^+ & \sqrt{2}K^+ \\ \sqrt{2}\pi^- & -\pi^0 + \frac{1}{\sqrt{3}}a\eta + \sqrt{\frac{2}{3}}b\eta' & \sqrt{2}K^0 \\ \sqrt{2}K^- & \sqrt{2}\bar{K}^0 & -\frac{2}{\sqrt{3}}b\eta + \sqrt{\frac{2}{3}}a\eta' \end{pmatrix}, \tag{9}$$

and

$$a = \cos\theta - \sqrt{2}\sin\theta\,, \qquad \sqrt{2}b = \sin\theta + \sqrt{2}\cos\theta\,. \tag{10}$$

θ is the $\eta - \eta'$ mixing angle. Note that we treat the singlet as a dynamical degree of freedom and include in Eq. (7) a term for the strong anomaly proportional to the instanton parameter α. This term gives a non-vanishing mass of the η_0 in the chiral limit ($m_q = 0$) reflecting the explicit breaking of the axial $U(1)$ symmetry. We shall keep the singlet term throughout the calculation and will discuss its effects in Section 6.

[2] In addition, one might note that the contribution of the contact term $\propto \langle\mathcal{M}^\dagger\mathcal{M}\rangle$ vanishes in the isospin limit ($m_u = m_d$).

The bosonic representation of the quark densities is defined in terms of (functional) derivatives:

$$\begin{aligned}(D_L)_{ij} &= \bar{q}_i \frac{1}{2}(1-\gamma_5) q_j \\ &\equiv -\frac{\delta \mathcal{L}_{eff}}{\delta \mathcal{M}_{ij}} = -r\Big(\frac{f^2}{4} U^\dagger + L_5 \partial_\mu U^\dagger \partial^\mu U U^\dagger + 2 r L_8 U^\dagger \mathcal{M} U^\dagger + r H_2 \mathcal{M}^\dagger\Big)_{ji}\,, \quad (11)\end{aligned}$$

and the right-handed density $(D_R)_{ij}$ is obtained by hermitian conjugation. Eq. (11) allows us to express the operators Q_6 and Q_8 in terms of the meson fields:

$$\begin{aligned}Q_6 &= -2 f^2 r^2 \sum_q \Big[\frac{1}{4} f^2 (U^\dagger)_{dq}(U)_{qs} + (U^\dagger)_{dq}(L_5 U \partial_\mu U^\dagger \partial^\mu U + 2 r L_8 U \mathcal{M}^\dagger U \\ &\quad + r H_2 \mathcal{M})_{qs} + (L_5 U^\dagger \partial_\mu U \partial^\mu U^\dagger + 2 r L_8 U^\dagger \mathcal{M} U^\dagger + r H_2 \mathcal{M}^\dagger)_{dq}(U)_{qs}\Big] + \mathcal{O}(p^4)\,, \quad (12)\end{aligned}$$

$$\begin{aligned}Q_8 &= -3 f^2 r^2 \sum_q e_q \Big[\frac{1}{4} f^2 (U^\dagger)_{dq}(U)_{qs} + (U^\dagger)_{dq}(L_5 U \partial_\mu U^\dagger \partial^\mu U + 2 r L_8 U \mathcal{M}^\dagger U \\ &\quad + r H_2 \mathcal{M})_{qs} + (L_5 U^\dagger \partial_\mu U \partial^\mu U^\dagger + 2 r L_8 U^\dagger \mathcal{M} U^\dagger + r H_2 \mathcal{M}^\dagger)_{dq}(U)_{qs}\Big] + \mathcal{O}(p^4). \quad (13)\end{aligned}$$

For the operator Q_6 the $(U^\dagger)_{dq}(U)_{qs}$ term which is of $\mathcal{O}(p^0)$ vanishes at the tree level. This property follows from the unitarity of U. However, when investigating off-shell corrections it must be included. This important aspect, which was not studied previously, will be discussed in detail in the following sections.

The $1/N_c$ corrections to the matrix elements $\langle Q_i \rangle_I$ are calculated by chiral loop diagrams. The diagrams are ultraviolet divergent and are regularized by a finite cutoff. This procedure, which was introduced in Ref. [1], is necessary in order to restrict the chiral lagrangian to the low-energy domain. Since we truncate the effective theory to pseudoscalar mesons, the cutoff has to be taken at or, preferably, below the $\mathcal{O}(1\ \mathrm{GeV})$. This limitation is a common feature of the various phenomenological approaches, which at present do not include higher resonances.

The loop expansion of the matrix elements is a series in $1/f^2 \sim 1/N_c$, which is in direct correspondence with the short-distance expansion in terms of $\alpha_s/\pi \sim 1/N_c$: the large-N_c behaviour of $SU(N_c)$ quantum chromodynamics is represented by diagrams which have a planar gluon structure. Subleading terms in the $1/N_c$ expansion are included by means of internal fermion loops (suppressed by a factor $1/N_c$) or non-planar gluon interactions (suppressed by $1/N_c^2$) [15]. These corrections actually generate the multimeson intermediate states which constitute the loop diagrams of the effective theory.[3]

[3] A pedagogical introduction to the $1/N_c$ expansion in terms of mesonic degrees of freedom can be found in Ref. [16].

Finally, we note that the meson loop corrections are needed not only for improving the matching of the matrix elements to the short-distance coefficient functions but also for obtaining the correct infrared structure, which is required to maintain the unitarity relations at low energy [17, 18].

3 Matching of Long and Short Distance

To calculate the amplitudes we follow the lines of Ref. [1] and identify the ultraviolet cutoff of the long-distance terms with the short-distance renormalization scale μ. In carrying out this matching we pay special attention to the definition of the momenta inside the loop. This question must be addressed because the loop integrals, within the cutoff regularization, are not momentum translation invariant.

In the existing studies of the hadronic matrix elements the color singlet boson connecting the two densities (or currents) was integrated out from the beginning [1, 2, 3, 4]. Thus the integration variable was taken to be the momentum of the meson in the loop, and the cutoff was the upper limit of its momentum. As there is no corresponding quantity in the short-distance part, in this treatment of the integrals there is no clear matching with QCD.

The ambiguity is removed, for non-factorizable diagrams, by considering the two densities to be connected to each other through the exchange of the color singlet boson, as was already discussed in Ref. [18]. A consistent matching is then obtained by assigning the same momentum to the color singlet boson at long and short distances and by identifying this momentum with the loop integration variable. This important feature of the modified approach is illustrated in Fig. 1. The momentum of the virtual meson is shifted by the external momentum, which affects both the ultraviolet, as well as, the infrared structure of the $1/N_c$ corrections. The same method was used in studies of the $K_L - K_S$ mass difference [19] and the evolution of current$\times$current operators in the chiral limit [20].

Obviously, the modified procedure described above is not applicable to the factorizable part of the interaction. However, in the next section we will show explicitly that all factorizable terms quadratic and logarithmic in the cutoff are independent of the momentum prescription in the loop. Moreover, they are absorbed in the renormalization of the bare low-energy coefficients, as well as the mesonic wave functions and masses. Consequently, the factorizable $1/N_c$ corrections are not to be matched to any short-distance contribution, i.e., they refer to the strong sector of the theory. Therefore there is no need for a momentum cutoff, and we will calculate the remaining finite corrections using dimensional regularization, which constitutes a momentum invariant procedure.

4 Factorizable $1/N_c$ Corrections

Since factorizable and non-factorizable corrections refer to disconnected sectors of the theory (strong and weak sectors), we introduce two different scales: λ_c is the cutoff for the factorizable diagrams and Λ_c for the non-factorizable. We will refer to them as the factorizable and the non-factorizable scales, respectively. A similar analysis of chiral loop corrections was performed to determine the B_K parameter [21].

We shall prove in this section, within the cutoff regularization, that the quadratic and logarithmic dependence on λ_c which arises from the factorizable loop diagrams is absorbed in the renormalization of the low-energy lagrangian. Consequently, in the factorizable sector the chiral loop corrections do not induce ultraviolet divergent terms, i.e., the only remaining ultraviolet structure of the matrix elements is contained in the overall factor $\sim 1/m_s^2$. This is to be expected as the evolution of m_s, which already appears at leading N_c, is the inverse of the evolution of a quark density. Therefore, except for the scale of $1/m_s^2$ which exactly cancels the factorizable evolution of the density$\times$density operators at short distances, the only scale remaining in the matrix elements is the non-factorizable scale Λ_c. It represents the non-trivial part of the factorization scale in the operator product expansion. Since the cutoff λ_c disappears through renormalization, the only matching between long- and short-distance contributions is obtained by identifying the cutoff scale Λ_c of the non-factorizable diagrams with the QCD renormalization scale μ.

The proof of the absorption of the factorizable scale λ_c will be carried out in the isospin limit. This explicit demonstration is instructive for several reasons. First, we verify the validity of the general concept in the case of bosonized densities which, contrary to the currents, do not obey conservation laws. Second, we check, within the cutoff formalism, whether there is a dependence on a given momentum shift ($q \to q \pm p$). Thirdly, including the η_0 as a dynamical degree of freedom we examine the corresponding modifications in the renormalization procedure. Finally, there remain finite terms from the factorizable $1/N_c$ corrections which explicitly enter the numerical analysis of the matrix elements. This point will be discussed at the end of this section.

4.1 Calculation of the Matrix Elements

Due to the unitarity of the matrix field U the tree level expansion of Q_6 starts at the $\mathcal{O}(p^2)$. Consequently, including only the first order corrections in the twofold expansion in external momenta and the ratio $1/N_c$, no additional terms arise from the renormalization of the wave functions and masses, as well as, the bare decay constant f since these corrections

will be of higher order. This statement does not hold for the electroweak operator Q_8 which, for $K^0 \to \pi^+\pi^-$, induces a non-vanishing tree matrix element at the $\mathcal{O}(p^0)$.

The wave function and mass renormalizations can be deduced from the pion and kaon self-energies, i.e., from a calculation of the propagators at next-to-leading order in the double series expansion. For the wave functions we obtain (defining $\pi_r \equiv Z_\pi^{1/2}\pi_0$)

$$Z_\pi = 1 + \frac{8L_5}{f^2}m_\pi^2 - \frac{\lambda_c^2}{(4\pi)^2 f^2} + \frac{m_K^2}{3(4\pi)^2 f^2}\log\left(1+\frac{\lambda_c^2}{m_K^2}\right) + \frac{2m_\pi^2}{3(4\pi)^2 f^2}\log\left(1+\frac{\lambda_c^2}{m_\pi^2}\right) \quad (14)$$

$$= 1 + \frac{8L_5}{f^2}m_\pi^2 - \frac{\lambda_c^2}{(4\pi)^2 f^2} + \frac{\log\lambda_c^2}{(4\pi)^2 f^2}\frac{1}{3}(m_K^2 + 2m_\pi^2) + \cdots\,, \quad (15)$$

$$Z_K = 1 + \frac{8L_5}{f^2}m_K^2 - \frac{\lambda_c^2}{(4\pi)^2 f^2} + \frac{1}{4(4\pi)^2 f^2}\left[m_\pi^2\log\left(1+\frac{\lambda_c^2}{m_\pi^2}\right) + 2m_K^2\log\left(1+\frac{\lambda_c^2}{m_K^2}\right)\right.$$
$$\left. + \cos^2\theta\; m_\eta^2\log\left(1+\frac{\lambda_c^2}{m_\eta^2}\right) + \sin^2\theta\; m_{\eta'}^2\log\left(1+\frac{\lambda_c^2}{m_{\eta'}^2}\right)\right] \quad (16)$$

$$= 1 + \frac{8L_5}{f^2}m_K^2 - \frac{\lambda_c^2}{(4\pi)^2 f^2} + \frac{\log\lambda_c^2}{(4\pi)^2 f^2}\frac{1}{6}(5m_K^2 + m_\pi^2) + \cdots\,, \quad (17)$$

where the ellipses denote finite terms we omit here for the analysis of the ultraviolet behaviour. One might note that Eqs. (14) and (16) are exact only if the cutoff is associated to the virtual meson. However, any momentum shift ($q \to q \pm p$) modifies only the finite corrections (compare Eq. (69) of Appendix B).

In specifying Eq. (17) we applied the octet-singlet squared mass matrix,

$$m^2 = \frac{1}{3}\begin{pmatrix} 4m_K^2 - m_\pi^2 & -2\sqrt{2}(m_K^2 - m_\pi^2) \\ -2\sqrt{2}(m_K^2 - m_\pi^2) & 2m_K^2 + m_\pi^2 + 3\alpha \end{pmatrix}, \quad (18)$$

with $\alpha = m_\eta^2 + m_{\eta'}^2 - 2m_K^2$ and the corresponding mixing angle [22]

$$\tan 2\theta = \frac{2m_{80}^2}{m_{00}^2 - m_{88}^2} = 2\sqrt{2}\left[1 - \frac{3\alpha}{2(m_K^2 - m_\pi^2)}\right]^{-1}. \quad (19)$$

The mass renormalization is found to be

$$m_\pi^2 = r\hat{m}\left[1 - \frac{8m_\pi^2}{f^2}(L_5 - 2L_8) + \frac{1}{3}\alpha\frac{\log\lambda_c^2}{(4\pi)^2 f^2}\right] + \cdots\,, \quad (20)$$

$$m_K^2 = r\frac{\hat{m} + m_s}{2}\left[1 - \frac{8m_K^2}{f^2}(L_5 - 2L_8) + \frac{1}{3}\alpha\frac{\log\lambda_c^2}{(4\pi)^2 f^2}\right] + \cdots\,, \quad (21)$$

where $\hat{m} = (m_u + m_d)/2$. The ratio of Eqs. (20) and (21), to one-loop order, determines the difference $L_5 - 2L_8$ of the low-energy couplings:

$$\frac{m_K^2}{m_\pi^2} = \frac{\hat{m}+m_s}{2\hat{m}}\left[1 - \frac{8(m_K^2-m_\pi^2)}{f^2}(L_5 - 2L_8)\right] + \cdots , \tag{22}$$

$$\equiv \frac{\hat{m}+m_s}{2\hat{m}}\left[1 - \frac{8(m_K^2-m_\pi^2)}{F_\pi^2}(\hat{L}_5^r - 2\hat{L}_8^r)\right] . \tag{23}$$

Note that Eq. (22) exhibits no explicit dependence on the scale λ_c; i.e., the chiral loop corrections of Eqs. (20) and (21) do not contribute to the $SU(3)$ breaking in the masses and, consequently, can be absorbed in r. This implies (modulo finite terms)

$$L_5 - 2L_8 = \hat{L}_5^r - 2\hat{L}_8^r . \tag{24}$$

Finally, f and L_5 are obtained from the decay constants of pions and kaons [1],

$$F_\pi = f\left[1 + \frac{4L_5}{f^2}m_\pi^2 - \frac{3}{2}\frac{\lambda_c^2}{(4\pi)^2 f^2} + \frac{\log\lambda_c^2}{(4\pi)^2 f^2}\frac{1}{2}(m_K^2 + 2m_\pi^2)\right] + \cdots , \tag{25}$$

$$F_K = f\left[1 + \frac{4L_5}{f^2}m_K^2 - \frac{3}{2}\frac{\lambda_c^2}{(4\pi)^2 f^2} + \frac{\log\lambda_c^2}{(4\pi)^2 f^2}\frac{1}{4}(5m_K^2 + m_\pi^2)\right] + \cdots . \tag{26}$$

Defining the constant $\hat{L}_5^r$ through the relation

$$\frac{F_K}{F_\pi} \equiv 1 + \frac{4\hat{L}_5^r}{F_\pi^2}(m_K^2 - m_\pi^2) , \tag{27}$$

from Eqs. (25) and (26) we find, to one-loop order,

$$L_5 = \hat{L}_5^r - \frac{3}{16}\frac{\log\lambda_c^2}{(4\pi)^2} + \cdots , \tag{28}$$

which is in accordance with the result from chiral perturbation theory [14]. Then, from Eq. (24) we get

$$L_8 = \hat{L}_8^r - \frac{3}{32}\frac{\log\lambda_c^2}{(4\pi)^2} + \cdots . \tag{29}$$

One might note that the coefficient in front of the logarithm in Eq. (29) differs from the one given in Ref. [14]. This property follows from the presence of the singlet η_0 in the calculation. Eqs. (22) and (23) define the renormalization conditions because the term $\hat{L}_5^r - 2\hat{L}_8^r$ plus the constant terms which appear in the ratio of the masses in Eq. (22) determine the bare constant $L_5 - 2L_8$. Similarly Eqs. (25)–(27) with the associated finite terms determine the coupling constant L_5. As we focus in this section on the ultraviolet

behaviour we omit the finite contributions. Full expressions relevant for the numerical analysis are given in terms of integrals in Appendix A.

Next we investigate the (bare) tree level of the $K^0 \to \pi\pi$ matrix elements, up to $\mathcal{O}(p^2)$ in the chiral expansion, as well as, the factorizable $1/N_c$ corrections to the $\mathcal{O}(p^0)$. The latter corrections refer to the first term on the right-hand side of Eqs. (12) and (13). Both contributions can be calculated from the diagrams depicted in Fig. 2. From the sum of these diagrams we obtain

$$i\langle \pi^0\pi^0|Q_6|K^0\rangle^F_{(0)} = -\frac{4\sqrt{2}}{f}r^2(m_K^2-m_\pi^2)\left[L_5+\frac{3}{16}\frac{\log\lambda_c^2}{(4\pi)^2}\right]+\cdots, \tag{30}$$

$$i\langle \pi^+\pi^-|Q_6|K^0\rangle^F_{(0)} = -\frac{4\sqrt{2}}{f}r^2(m_K^2-m_\pi^2)\left[L_5+\frac{3}{16}\frac{\log\lambda_c^2}{(4\pi)^2}\right]+\cdots, \tag{31}$$

$$i\langle \pi^0\pi^0|Q_8|K^0\rangle^F_{(0)} = \frac{2\sqrt{2}}{f}r^2(m_K^2-m_\pi^2)\left[L_5+\frac{3}{16}\frac{\log\lambda_c^2}{(4\pi)^2}\right]+\cdots, \tag{32}$$

$$\begin{aligned} i\langle \pi^+\pi^-|Q_8|K^0\rangle^F_{(0)} &= \frac{3}{4}\sqrt{2}r^2 f\left[1-\frac{4}{3f^2}(m_K^2+2m_\pi^2)(L_5-12L_8)-\frac{3\lambda_c^2}{(4\pi)^2f^2}\right.\\ &\left.+\frac{1}{12}\frac{\log\lambda_c^2}{(4\pi)^2f^2}(21m_K^2+24m_\pi^2+8\alpha)\right]+\cdots. \end{aligned} \tag{33}$$

The structure of Eqs. (30)–(32) guarantees that the renormalization of L_5 renders them finite. The situation is more complicated for the matrix element in Eq. (33) as we will remark below.

If we use Eqs. (15)–(29), including only the first order corrections in the parameter expansion, we arrive at the renormalized (factorizable) matrix elements of the Q_6 and Q_8 operators:[4]

$$i\langle \pi^0\pi^0|Q_6|K^0\rangle^F_{(r)} = -\frac{4\sqrt{2}}{F_\pi}\left(\frac{2m_K^2}{\hat{m}+m_s}\right)^2(m_K^2-m_\pi^2)\hat{L}_5^r+\cdots, \tag{34}$$

$$i\langle \pi^+\pi^-|Q_6|K^0\rangle^F_{(r)} = -\frac{4\sqrt{2}}{F_\pi}\left(\frac{2m_K^2}{\hat{m}+m_s}\right)^2(m_K^2-m_\pi^2)\hat{L}_5^r+\cdots, \tag{35}$$

$$i\langle \pi^0\pi^0|Q_8|K^0\rangle^F_{(r)} = \frac{2\sqrt{2}}{F_\pi}\left(\frac{2m_K^2}{\hat{m}+m_s}\right)^2(m_K^2-m_\pi^2)\hat{L}_5^r+\cdots, \tag{36}$$

$$i\langle \pi^+\pi^-|Q_8|K^0\rangle^F_{(r)} = \frac{3}{4}\sqrt{2}\left(\frac{2m_K^2}{\hat{m}+m_s}\right)^2\left[F_\pi+\frac{4}{3F_\pi}(8m_K^2-11m_\pi^2)\hat{L}_5^r\right.$$

[4] L_8 does not appear in the matrix elements of Q_6 because its contributions to the first and second diagram of Fig. 2 are canceled by a tadpole (third diagram of Fig. 2).

$$-\frac{16}{F_\pi}(m_K^2-2m_\pi^2)\hat{L}_8^r\Bigg]+\cdots\ . \tag{37}$$

Eqs. (34)–(37) are unambiguous, as the quadratic and logarithmic terms in Eqs. (15)–(33) were found to be independent of the momentum prescription inside the loops.

Note that the factorizable scale λ_c is absent in Eqs. (34)–(37) [except for the running of $1/(\hat{m}+m_s)^2 \simeq 1/m_s^2$]. Residual scale dependences could nevertheless unfold at the orders p^0/N_c^2 or p^2/N_c. The latter would arise, e.g., if we used f rather than F_π in the $\mathcal{O}(p^2)$ tree level expressions of Eqs. (23) and (27) or Eqs. (34)–(37). This would be consistent at the level of the first order corrections in the twofold series expansion, as the difference concerns higher order effects. However, the scale dependence of f (which is mainly quadratic) will be absorbed by factorizable loop corrections to the matrix elements at the next order in the parameter expansion and has not to be matched to any short-distance contribution. Consequently, it is a more adequate choice to use the physical decay constant in the expressions under consideration. Instead of F_π the kaon decay constant F_K could be used as well. Both choices will be considered in the numerical analysis, which gives a rough estimate of higher order corrections. At the same level of accuracy, in the $\mathcal{O}(p^2)$ terms of Eqs. (34)–(37) the prefactor $[2m_K^2/(\hat{m}+m_s)]^2$ could be replaced by $(m_\pi^2/\hat{m})^2$. However, this choice is unsuitable as $\hat{m}$ suffers from larger uncertainties.

We note that the coefficients in front of $\hat{L}_5^r$ and $\hat{L}_8^r$ in the matrix element of Eq. (37) are different from those of the bare couplings L_5 and L_8 in Eq. (33). The change of the coefficients comes about as the quantities in Eq. (33) are replaced by renormalized quantities. In particular, the quadratic term in λ_c is absorbed in the renormalization of the decay constant f and the mesonic wave functions. Finally, omitting the constant terms which refer to the factorizable loop corrections, Eqs. (36) and (37) are combined to obtain the isospin-two tree level matrix element of Q_8 up to $\mathcal{O}(p^2)$ in the chiral expansion:

$$i\langle Q_8\rangle_2^{tree}=\frac{\sqrt{3}}{2\sqrt{2}}\left(\frac{2m_K^2}{\hat{m}+m_s}\right)^2\left[F_\pi+\frac{4}{F_\pi}(2m_K^2-3m_\pi^2)\hat{L}_5^r-\frac{16}{F_\pi}(m_K^2-2m_\pi^2)\hat{L}_8^r\right]. \tag{38}$$

The numerical value for this term is given in Table 1. In Ref. [23] only the bare matrix elements were included in the corresponding tree level analysis of $\langle Q_8\rangle_2$. Consequently, the new contribution of Ref. [23], i.e., the contribution of the L_8 coupling, was found with a sign opposite to that in Eq. (38). This was corrected in Ref. [24] in the framework of the chiral quark model.

4.2 Operator Evolution

The results of the previous section can also be seen directly at the operator level, in particular at the level of the density operator. To demonstrate this we apply the background field method as used in Refs. [20] and [25] for current×current operators. This approach is powerful as it keeps track of the chiral structure in the loop corrections. It is particularly useful to study the ultraviolet behaviour of the theory.

In order to calculate the evolution of the density operator we decompose the matrix U in the classical field $\bar{U}$ and the quantum fluctuation ξ,

$$U = \exp(i\xi/f)\,\bar{U}\ , \quad \xi = \xi^a\lambda_a\,, \tag{39}$$

with $\bar{U}$ satisfying the equation of motion

$$\bar{U}\partial^2\bar{U}^\dagger - \partial^2\bar{U}\bar{U}^\dagger + r\bar{U}\mathcal{M}^\dagger - r\mathcal{M}\bar{U}^\dagger = \frac{\alpha}{N_c}\langle\ln\bar{U} - \ln\bar{U}^\dagger\rangle\cdot\mathbf{1}\ , \quad \bar{U} = \exp(i\pi^a\lambda_a/f)\ . \tag{40}$$

The lagrangian of Eq. (7) thus reads

$$\mathcal{L} = \bar{\mathcal{L}} + \frac{1}{2}(\partial_\mu\xi^a\partial^\mu\xi_a) + \frac{1}{4}\langle[\partial_\mu\xi,\,\xi]\partial^\mu\bar{U}\bar{U}^\dagger\rangle - \frac{r}{8}\langle\xi^2\bar{U}\mathcal{M}^\dagger + \bar{U}^\dagger\xi^2\mathcal{M}\rangle - \frac{1}{2}\alpha\xi^0\xi^0 + \mathcal{O}(\xi^3)\ . \tag{41}$$

The corresponding expansion of the meson density around the classical field yields

$$(D_L)_{ij} = (\bar{D}_L)_{ij} + if\frac{r}{4}(\bar{U}^\dagger\xi)_{ji} + \frac{r}{8}(\bar{U}^\dagger\xi^2)_{ji} + \mathcal{O}(\xi^3)\ . \tag{42}$$

The evolution of $(D_L)_{ij}$ is determined by the diagrams of Fig. 4, and we obtain

$$\begin{aligned}(D_L)_{ij}(\lambda_c) \;=\; & -\frac{f^2}{4}r(\bar{U}^\dagger)_{ji}(0) + \frac{3}{4}r(\bar{U}^\dagger)_{ji}(0)\frac{\lambda_c^2}{(4\pi)^2} - \frac{r}{12}(\bar{U}^\dagger)_{ji}(0)\alpha\frac{\log\lambda_c^2}{(4\pi)^2} \\ & -r^2(\mathcal{M}^\dagger)_{ji}(0)\left[H_2 + \frac{3}{16}\frac{\log\lambda_c^2}{(4\pi)^2}\right] - 2r^2(\bar{U}^\dagger\mathcal{M}\bar{U}^\dagger)_{ji}(0)\left[L_8 + \frac{3}{32}\frac{\log\lambda_c^2}{(4\pi)^2}\right] \\ & -r(\partial_\mu\bar{U}^\dagger\partial^\mu\bar{U}\bar{U}^\dagger)_{ji}(0)\left[L_5 + \frac{3}{16}\frac{\log\lambda_c^2}{(4\pi)^2}\right]\ .\end{aligned} \tag{43}$$

The quadratic and logarithmic terms for the wave function and mass renormalizations can be calculated from the diagrams of Figs. 6 and 7, i.e., from the off-shell corrections to the kinetic and the mass operator, respectively, second and third term of Eq. (41). The resulting expressions for m_π^2 and m_K^2 turn out to be identical to those found in the explicit calculation of the pion and kaon self-energies, Eqs. (20) and (21). For the wave functions we get

$$Z_\pi \;=\; 1 + \frac{8L_5}{f^2}m_\pi^2 - 3\frac{\lambda_c^2}{(4\pi)^2f^2} + \frac{3}{2}m_\pi^2\frac{\log\lambda_c^2}{(4\pi)^2f^2}\,, \tag{44}$$

$$Z_K \;=\; 1 + \frac{8L_5}{f^2}m_K^2 - 3\frac{\lambda_c^2}{(4\pi)^2f^2} + \frac{3}{2}m_K^2\frac{\log\lambda_c^2}{(4\pi)^2f^2}\,. \tag{45}$$

Along the same lines F_π and F_K can be calculated, to one-loop order, from the diagrams of Fig. 5, and we obtain[5]

$$F_\pi = f\left[1+\frac{4L_5}{f^2}m_\pi^2-\frac{3}{2}\frac{\lambda_c^2}{(4\pi)^2f^2}+\frac{3}{4}m_\pi^2\frac{\log\lambda_c^2}{(4\pi)^2f^2}\right], \tag{46}$$

$$F_K = f\left[1+\frac{4L_5}{f^2}m_K^2-\frac{3}{2}\frac{\lambda_c^2}{(4\pi)^2f^2}+\frac{3}{4}m_K^2\frac{\log\lambda_c^2}{(4\pi)^2f^2}\right]. \tag{47}$$

In accordance with Eqs. (15)–(33) both the quadratic and the logarithmic terms of Eqs. (43)–(47) prove to be independent of the way we define the integration variable inside the loops. This is due to the fact that the quadratically divergent integrals resulting from the diagrams of Figs. 4-7 [i.e., those of the form $d^4q/(q\pm p)^2$] do not induce subleading logarithms, that is to say, all quadratic and logarithmic dependence on the scale λ_c originates from the leading divergence of a given integral.

Now looking at Eqs. (44)–(47) we observe that the ratio Π/f and, consequently, the matrix field U are not renormalized (i.e., $\pi_0/f=\pi_r/F_\pi$ and $K_0/f=K_r/F_K$). Then, by means of Eqs. (21) and (46), we can rewrite the density of Eq. (43) as

$$\begin{aligned}(D_L)_{ij}(\lambda_c) &= -\frac{2m_K^2}{(\hat m+m_s)}\left[\frac{F_\pi^2}{4}\left(1+\frac{8\hat L_5^r}{F_\pi^2}\left(m_K^2-m_\pi^2\right)-\frac{16\hat L_8^r}{F_\pi^2}m_K^2\right)(\bar U^\dagger)_{ji}\right.\\ &\left.+(\partial_\mu\bar U^\dagger\partial^\mu\bar U\bar U^\dagger)_{ji}\hat L_5^r+2(\bar U^\dagger\chi\bar U^\dagger)_{ji}\hat L_8^r+(\chi^\dagger)_{ji}\hat H_2^r\right],\end{aligned} \tag{48}$$

with $\chi=\mathrm{diag}(m_\pi^2,\,m_\pi^2,\,2m_K^2-m_\pi^2)$. In obtaining Eq. (48) we used the renormalized couplings of Eqs. (28) and (29). In addition, we introduced

$$\hat H_2^r = H_2+\frac{3}{16}\frac{\log\lambda_c^2}{(4\pi)^2}+\cdots\ . \tag{49}$$

Note that the renormalized density exhibits no dependence on the scale λ_c, except for the scale of $1/(\hat m+m_s)$. Note also that in Eqs. (43) and (48) we did not specify logarithmic terms induced at the one-loop order which correspond to the L_4, L_6 and L_7 operators in the chiral effective lagrangian of Ref. [14]. An explicit calculation of these terms shows that they give no contribution to the $K\to\pi\pi$ matrix elements of Q_6 and Q_8.

In conclusion, using a cutoff regularization the factorizable contributions to the Q_6 and Q_8 operators up to the orders p^2 and p^0/N_c are given, modulo finite loop corrections, in terms of the $K\to\pi\pi$ matrix elements by Eqs. (34)–(37) or in terms of a single density by Eq. (48). Our results exhibit no explicit scale dependence. Moreover, they do not depend

[5]The representation of the bosonized current in terms of the background field can be found in Ref. [20].

on the momentum prescription inside the loops. The finite terms, on the other hand, will not be absorbed completely in the renormalization of the various parameters. This can be seen, e.g., from the fact that the rescattering diagrams of Fig. 2 contain a non-vanishing imaginary part. As the renormalized parameters are defined to be real, the latter will remain.

In addition, the real part of the finite corrections carries a dependence on the momentum prescription used to define the cutoff. However, we proved that the chiral loop diagrams do not induce ultraviolet divergent terms. Therefore we are allowed to calculate the remaining finite corrections in dimensional regularization, which is momentum translation invariant (i.e., we are allowed to take the limit $\lambda_c \to \infty$). This procedure implies an extrapolation of the low-energy effective theory for terms of $\mathcal{O}(m_{\pi,K}^2/\lambda_c^2;\ m_{\pi,K}^4/\lambda_c^4;\ \ldots)$ up to scales where these terms are negligible. This is the usual assumption made in chiral perturbation theory for three flavors.

5 Non-factorizable $1/N_c$ Corrections

The non-factorizable $1/N_c$ corrections to the hadronic matrix elements constitute the part to be matched to the short-distance Wilson coefficient functions; i.e., the corresponding scale Λ_c has to be identified with the renormalization scale μ of QCD. We perform this identification, as we argued in Section 3, by associating the cutoff to the effective color singlet boson. Then, at the $\mathcal{O}(p^0)$ in the chiral expansion of the Q_6 and Q_8 operators, from the diagrams of Fig. 3 we obtain

$$i\langle\pi^0\pi^0|Q_6|K^0\rangle^{NF} = \sqrt{2}\frac{3}{4}\left(\frac{2m_K^2}{\hat{m}+m_s}\right)^2\frac{1}{F_\pi}\frac{\log\Lambda_c^2}{(4\pi)^2}(m_K^2-m_\pi^2)+\cdots, \tag{50}$$

$$i\langle\pi^+\pi^-|Q_6|K^0\rangle^{NF} = \sqrt{2}\frac{3}{4}\left(\frac{2m_K^2}{\hat{m}+m_s}\right)^2\frac{1}{F_\pi}\frac{\log\Lambda_c^2}{(4\pi)^2}(m_K^2-m_\pi^2)+\cdots, \tag{51}$$

$$i\langle\pi^0\pi^0|Q_8|K^0\rangle^{NF} = \sqrt{2}\frac{3}{4}\left(\frac{2m_K^2}{\hat{m}+m_s}\right)^2\frac{1}{F_\pi}\frac{\log\Lambda_c^2}{(4\pi)^2}(m_K^2-m_\pi^2)+\cdots, \tag{52}$$

$$i\langle\pi^+\pi^-|Q_8|K^0\rangle^{NF} = -\frac{\sqrt{2}}{2}\left(\frac{2m_K^2}{\hat{m}+m_s}\right)^2\frac{1}{F_\pi}\frac{\log\Lambda_c^2}{(4\pi)^2}\alpha+\cdots. \tag{53}$$

Again, for the reason of brevity in Eqs. (50)–(53) we did not specify the finite terms which must be included in the numerical analysis (in particular, they provide the reference scale for the logarithms). In addition, we replaced m_η^2, $m_{\eta'}^2$ and the mixing angle θ by m_π^2, m_K^2 and the instanton parameter α using the octet-singlet mass matrix of Eq. (18).

Note that in Eqs. (50)–(53) we used $1/F_\pi$ and $2m_K^2/(\hat{m}+m_s)$ rather than the bare parameters $1/f$ and r. Again the difference represents higher order effects. However, the appearance of f or r in Eqs. (50)–(53) would induce a dependence on the factorizable scale λ_c, which has no counterpart in the short-distance domain (compare the discussion at the end of Section 4.1). As for the factorizable contributions the choice of F_K instead of F_π would be also appropriate.

The results presented above are in accordance with the non-factorizable evolution of Q_6 and Q_8 we obtain in the background field approach by calculating the diagrams of Fig. 8:

$$\begin{aligned} Q_6^{NF}(\Lambda_c^2) &= F_\pi^2 \left(\frac{2m_K^2}{\hat{m}+m_s}\right)^2 \frac{\log\Lambda_c^2}{(4\pi)^2}\Big[\frac{3}{4}(\partial_\mu \bar{U}^\dagger \partial^\mu \bar{U})_{ds} \\ &\quad + \frac{1}{2}(\partial_\mu \bar{U}^\dagger \bar{U})_{ds} \sum_q (\bar{U}\partial^\mu \bar{U}^\dagger)_{qq} + \frac{3}{4}(\bar{U}^\dagger\chi + \chi^\dagger \bar{U})_{ds}\Big], \end{aligned} \tag{54}$$

$$\begin{aligned} Q_8^{NF}(\Lambda_c^2) &= \frac{3}{2}F_\pi^2 \left(\frac{2m_K^2}{\hat{m}+m_s}\right)^2 \frac{\log\Lambda_c^2}{(4\pi)^2} \sum_q e_q \Big[\frac{1}{4}(\partial_\mu \bar{U}^\dagger \partial^\mu \bar{U})_{ds}\delta_{qq} \\ &\quad + \frac{1}{2}(\partial_\mu \bar{U}^\dagger \bar{U})_{ds}(\bar{U}\partial^\mu \bar{U}^\dagger)_{qq} + \frac{1}{4}(\bar{U}^\dagger\chi + \chi^\dagger\bar{U})_{ds}\delta_{qq} + \frac{1}{3}\alpha(\bar{U}^\dagger)_{dq}(\bar{U})_{qs}\Big]. \end{aligned} \tag{55}$$

Only the diagonal evolution of Q_6, i.e., the first term on the right-hand side of Eq. (54), gives a non-zero contribution to the matrix elements of Eqs. (50) and (51). In particular, the mass term which is of the L_8 and H_2 form vanishes for $K \to \pi\pi$ decays, as do the L_8 and H_2 contributions at the tree level (see Section 4). In Eq. (55) for completeness we kept the terms proportional to δ_{qq} which, however, cancel through the summation over the flavor index.

Note that Eqs. (54) and (55) are given in terms of operators and, consequently, can be applied to $K \to 3\pi$ decays, too. Note also that our results, Eqs. (50)–(55), exhibit no quadratic dependence on the scale Λ_c; i.e., up to the first order corrections in the twofold series expansion the matching involves only logarithmic terms from both the short- *and* the long-distance evolution of the four-quark operators. This is due to the fact that there is no quadratically divergent diagram in Fig. 8 apart from the first one which vanishes for the Q_6 and Q_8 operators. Moreover, for a general density×density operator there are no logarithms which are the subleading logs of quadratically divergent terms. Therefore, all the logarithms appearing in Eqs. (50)–(55) are leading divergences, which are independent of the momentum prescription. The finite terms calculated along with these logarithms depend on the momentum prescription. They are, however, uniquely determined through the matching condition with QCD (see Fig. 1).

One might note that the statements we made above do not hold for current×current operators: the $1/N_c$ corrections to these operators, performed in the first non-vanishing order of their chiral expansion, exhibit terms which are quadratic in Λ_c. Furthermore, already these terms were shown to depend on the momentum prescription [20].

We close this section by giving the long-distance evolution, at the $\mathcal{O}(p^0)$, of a general density×density operator $Q_D^{abcd} \equiv -8(D_R)_{ab}(D_L)_{cd}$. As we showed in Section 4.2, the factorizable $1/N_c$ corrections do not affect its ultraviolet behaviour. Then, from the non-factorizable diagrams of Fig. 8 we find

$$\begin{aligned} Q_D^{abcd}(\Lambda_c^2) &= Q_D^{abcd}(0)\left[1-\frac{2}{3}\frac{\alpha}{F_\pi^2}\frac{\log\Lambda_c^2}{(4\pi)^2}\right] - F_\pi^2\left(\frac{2m_K^2}{\hat{m}+m_s}\right)^2\frac{\Lambda_c^2}{(4\pi)^2}\delta^{da}\delta^{bc} \\ &+\frac{F_\pi^2}{4}\left(\frac{2m_K^2}{\hat{m}+m_s}\right)^2\frac{\log\Lambda_c^2}{(4\pi)^2}\Big[(\bar{U}^\dagger\chi+\chi^\dagger\bar{U})^{da}\delta^{bc}+\delta^{da}(\chi\bar{U}^\dagger+\bar{U}\chi^\dagger)^{bc} \\ &+(\partial_\mu\bar{U}^\dagger\partial^\mu\bar{U})^{da}\delta^{bc}+\delta^{da}(\partial_\mu\bar{U}\partial^\mu\bar{U}^\dagger)^{bc}+2(\partial_\mu\bar{U}^\dagger\bar{U})^{da}(\bar{U}\partial^\mu\bar{U}^\dagger)^{bc}\Big]. \quad (56) \end{aligned}$$

The corresponding expressions for the non-factorizable loop corrections to operators Q_6 and Q_8, Eqs. (54) and (55), can be obtained directly from Eq. (56).

6 Numerical Analysis and Discussion of Results

To compute the hadronic matrix elements of Q_6 and Q_8 we pursued the following strategy. First, the non-factorizable contributions were calculated, in the isospin limit, from the diagrams of Fig. 3. In this part of the analysis the finite terms, which are systematically determined by the momentum prescription of Fig. 1, are completely taken into account. By using algebraic relations all integrals resulting from the diagrams of Fig. 3 can be reduced to three basic integrals which are given explicitly, in the framework of the cutoff regularization, in Appendix B. They were computed up to terms of the order p^4 and p^6, respectively, that is to say, to a relative precision of approximately 10^{-2}. Second, the finite terms arising from the factorizable loop diagrams of Fig. 2, as well as, from the renormalization of the wave functions, the masses and the low-energy couplings were estimated using dimensional regularization, as discussed at the end of Section 4.2.

We use the following numerical values for the parameters:

$$\begin{aligned} m_\pi &\equiv (m_{\pi^0}+m_{\pi^+})/2 = 137.3\ \text{MeV}, & F_\pi &= 92.4\ \text{MeV}, \\ m_K &\equiv (m_{K^0}+m_{K^+})/2 = 495.7\ \text{MeV}, & F_K &= 113\ \text{MeV}, \\ m_\eta &= 547.5\ \text{MeV}, & \theta &= -19^\circ, \\ m_{\eta'} &= 957.8\ \text{MeV}. \end{aligned}$$

Substituting them in Eqs. (23) and (27) we compute $\hat{L}_5^r = 2.07\times10^{-3}$ and $\hat{L}_8^r = 1.09\times10^{-3}$. For the numerical values given above, $\hat{L}_5^r$ is close to $2\hat{L}_8^r$, and we find the $\mathcal{O}(p^2)$ tree level contribution to $\langle Q_8\rangle_2$ to be small, because the term proportional to m_K^2 in Eq. (38) approximately vanishes. This result is different from the statements made in Ref. [23]. The full expressions needed for the renormalization of the parameters f, L_5 and L_8 in terms of integrals are presented in Appendix A. In the octet limit the results in the appendix are the same as in Refs. [14] and [26].[6] Finally, we used the ratio $m_s/\hat{m} = 24.4\pm1.5$ [27] which enters in the calculation of $\hat{L}_8^r$.

The values we obtain for the matrix elements of Q_6 and Q_8 are presented in Table 1, where we also specify the various contributions coming from the factorizable and the non-factorizable diagrams, respectively. In these matrix elements we have extracted the factor $R^2 = [2m_K^2/(\hat{m}+m_s)]^2$, whose dependence on the factorizable scale will be canceled exactly, for a general density×density operator, by the diagonal evolution of the Wilson coefficients. Finally, for comparison, we present in Table 1 also the numerical values obtained by replacing F_π by F_K in the $\mathcal{O}(p^2)$ and $\mathcal{O}(p^0/N_c)$ factorizable and non-factorizable contributions, that is to say, in the corresponding terms of Eqs. (23), (27) [or Eqs. (60)–(63) of Appendix A], (34)–(37) and (50)–(53), and in the finite terms. The difference gives a rough estimate of the higher order corrections.

In Table 2 we list the corresponding values for the B_i factors, which quantify the deviation of the hadronic matrix elements from the VSA results:

$$B_6^{(1/2)} = |\langle Q_6\rangle_0/\langle Q_6\rangle_0^{\rm VSA}|\,, \qquad B_8^{(3/2)} = |\langle Q_8\rangle_2/\langle Q_8\rangle_2^{\rm VSA}|\,. \tag{57}$$

The VSA expressions for the matrix elements were taken from Eqs. (XIX.16) and (XIX.24) of Ref. [28]. Numerically, they are $|\langle Q_6\rangle_0| = 35.2\cdot R^2\,\text{MeV}$ and $|\langle Q_8\rangle_2| = 56.6\,\text{MeV}\cdot[R^2 - (0.389\,\text{GeV})^2]$. The second term in the expression for Q_8 contributes at the 2 % level and has been neglected in Table 2.

We discuss next the corrections to the matrix elements $\langle Q_6\rangle_0$ and $\langle Q_8\rangle_2$. As already mentioned, the operator Q_6 is special because the $\mathcal{O}(p^0)$ tree level matrix element is zero due to the unitarity of the matrix U. Nevertheless the one-loop corrections to this matrix element must be computed. These corrections are of $\mathcal{O}(p^0/N_c)$ and are non-vanishing. We have shown in Eqs. (50) and (51) that the explicit calculation of the loops yields a cutoff dependence (i.e., a non-trivial scale dependence) from the non-factorizable diagrams which has to be matched to the short-distance contribution. In addition, the logarithms

[6] Note that our constants $\hat{L}_5^r$ and $\hat{L}_8^r$ should not be confused with the scale dependent coefficients L_5^r and L_8^r in Refs. [14] and [26].

	$\Lambda_c = 0.6$ GeV	$\Lambda_c = 0.7$ GeV	$\Lambda_c = 0.8$ GeV	$\Lambda_c = 0.9$ GeV
$i\langle Q_6\rangle_0^{\text{tree}}$	-35.2	-35.2	-35.2	-35.2
$i\langle Q_6\rangle_0^{\text{tree + F loops}}$	$-68.4 - 37.0i$	$-68.4 - 37.0i$	$-68.4 - 37.0i$	$-68.4 - 37.0i$
$i\langle Q_6\rangle_0^{\text{NF loops}}$	$29.8 + 37.0i$	$34.6 + 37.0i$	$39.0 + 37.0i$	$42.9 + 37.0i$
$\lvert\langle Q_6\rangle_0\rvert^{\text{total}}$	38.6	33.7	29.4	25.5
	(45.8)	(41.8)	(38.2)	(35.0)
$i\langle Q_8\rangle_2^{\text{tree}}$	56.4	56.4	56.4	56.4
$i\langle Q_8\rangle_2^{\text{tree + F loops}}$	$56.0 - 0.1i$	$56.0 - 0.1i$	$56.0 - 0.1i$	$56.0 - 0.1i$
$i\langle Q_8\rangle_2^{\text{NF loops}}$	$-20.7 - 11.5i$	$-24.8 - 11.5i$	$-28.8 - 11.5i$	$-32.8 - 11.5i$
$\lvert\langle Q_8\rangle_2\rvert^{\text{total}}$	37.2	33.2	29.5	25.9
	(40.2)	(37.0)	(33.8)	(30.7)

Table 1: Hadronic matrix elements of Q_6 and Q_8 (in units of $R^2 \cdot$ MeV), shown for various values of Λ_c. The numbers in the parentheses are obtained by replacing F_π by F_K in the next-to-leading order expressions.

of Eqs. (34) and (35) are needed in order to cancel the scale dependence of various bare parameters in the tree level expressions, as was checked explicitly in Section 4. We note that in the twofold expansion in p^2 and p^0/N_c the contribution of the loops over the $\mathcal{O}(p^0)$ matrix element must be treated at the same level as the leading non-vanishing tree contribution proportional to L_5. This is revealed by the large size of the non-factorizable $\mathcal{O}(p^0/N_c)$ corrections presented in Table 1. It is the sum of both, the factorizable and the non-factorizable contributions, which renders the numerical values for $\langle Q_6\rangle_0$ close to the VSA value. For the imaginary part, which is due to on-shell rescattering effects and does not depend on the matching condition with QCD (see Fig. 1), the cancellation is complete. This property follows from the $(U^\dagger)_{dq}(U)_{qs}$ structure of the operator. The main effect of the loop corrections is to change the dependence of $\langle Q_6\rangle_0$ on Λ_c, from a flat behaviour at the tree level to the dependence presented in Tables 1 and 2, which is important for the matching. We note that at $\Lambda_c \simeq 700$ MeV the value for the matrix element of Q_6 is very close to the VSA result leading to $B_6 \simeq 1$.

	$\Lambda_c = 0.6$ GeV	$\Lambda_c = 0.7$ GeV	$\Lambda_c = 0.8$ GeV	$\Lambda_c = 0.9$ GeV
$B_6^{(1/2)}$	1.10	0.96	0.84	0.72
	(1.30)	(1.19)	(1.09)	(0.99)
$B_8^{(3/2)}$	0.66	0.59	0.52	0.46
	(0.71)	(0.65)	(0.60)	(0.54)

Table 2: B_6 and B_8 factors for various values of the cutoff Λ_c.

The Q_8 operator is not chirally suppressed, i.e., its $\mathcal{O}(p^0)$ tree level matrix element is non-zero. In this article we include the tree level contribution up to $\mathcal{O}(p^2)$, as well as, the loop corrections of $\mathcal{O}(p^0/N_c)$, that is to say, corrections to the first term of Eq. (13). This is a full leading plus next-to-leading order analysis of the Q_8 matrix element. The one-loop corrections, even though suppressed by a factor $1/N_c$ with respect to the leading tree level, are found to be large and negative, leading to the small values for B_8 presented in Table 2. These large corrections persist in the octet limit [i.e, in the absence of the η_0, with $a = b = 1$ and $m_\eta^2 = (4m_K^2 - m_\pi^2)/3$]. Therefore, they are not due to the presence of the η_0 which brings in a small change. One might note that the numbers in Table 2 are specified for the central value of $m_s/\hat{m} = 24.4 \pm 1.5$ [27]. Including the error of this mass ratio changes the B_8 parameter by $\pm$ 0.06.

In comparison with $\langle Q_6 \rangle_0$, the non-factorizable corrections to $\langle Q_8 \rangle_2$ are less pronounced, as expected from the power counting scheme in p^2 and $1/N_c$. However, because the factorizable $\mathcal{O}(p^2)$ and $\mathcal{O}(p^0/N_c)$ corrections are small (and negative), the non-factorizable terms produce a significant reduction of $\langle Q_8 \rangle_2$. The size of the higher order terms indicates that the leading-N_c calculation or the closely related VSA are not sufficient for the matrix elements of the Q_8 operator.[7]

In view of the large corrections one might question the convergence of the $1/N_c$ expansion. However, there is no strong reason for such doubts because the non-factorizable contribution we consider in this paper represents the first term in a new type of a series absent in the large-N_c limit. It is reasonable to assume that this leading non-factorizable term carries a large fraction of the whole contribution.

As a general result, we note that our study indicates a significant reduction of $B_8^{(3/2)}$. By comparison the corrections to $B_6^{(1/2)}$ are moderate, i.e., there is no clear tendency for values

[7] This has already been observed for the matrix elements of Q_1 and Q_2 which are relevant for the $\Delta I = 1/2$ selection rule [1].

much larger or smaller than one. Our results for $\langle Q_6\rangle_0$ and $\langle Q_8\rangle_2$ can still be improved by calculating higher order terms in p^2 and $1/N_c$, like for instance those of $\mathcal{O}(p^2/N_c)$ which will be along the lines of this work. The $\mathcal{O}(p^2/N_c)$ will bring in a quadratic dependence on Λ_c [29] and even though suppressed by a factor of p^2 relative to the $\mathcal{O}(p^0/N_c)$ may compensate, to a large extent, the scale dependence of the logarithmic terms of this paper. Another improvement would be to include the vector mesons which is a new calculation beyond the scope of this work.

It is interesting to compare our results with those of other calculations. Refs. [3] and [4] investigated $1/N_c$ corrections to the matrix elements of Q_6 and Q_8. This calculation considered the product of the two densities without the color singlet boson and the matching of short- and long-distance contributions was not explicit as in the present article. The $\mathcal{O}(p^0/N_c)$ contribution to Q_6 was not included, but terms of $\mathcal{O}(p^2/N_c)$ were included in Q_6 and Q_8. In this study the parametrization of the $\mathcal{O}(p^4)$ lagrangian was not general as only one coupling constant was introduced. The numerical results showed also a tendency of reducing $\langle Q_8\rangle_2$ substantially, whereas $\langle Q_6\rangle_0$ was found to be enhanced compared to the VSA result. Calculations in lattice QCD obtain values for B_6 close to the VSA, $B_6^{(1/2)}(2\,\mathrm{GeV}) = 1.0 \pm 0.2$ [30, 31] and 0.76(3)(5) [32]. Recent values reported for B_8 are $B_8^{(3/2)}(2\,\mathrm{GeV}) = 0.81(3)(3)$ [33], 0.77(4)(4) [34], and 1.03(3) [35]. These studies use tree level chiral perturbation theory to relate the matrix elements $\langle\pi\pi|Q_i|K\rangle$ to $\langle\pi|Q_i|K\rangle$ which are calculated on the lattice. The chiral quark model [24] yields a range for B_6 which is above the VSA value, $B_6^{(1/2)}(0.8\,\mathrm{GeV}) = 1.2 - 1.9$, and predicts a small reduction of the B_8 factor, $B_8^{(3/2)}(0.8\,\mathrm{GeV}) = 0.91 - 0.94$. Although the scales used in the lattice calculations and the phenomenological approaches are different, the various results can be compared as the B_6 and B_8 parameters were shown in QCD to depend only very weakly on the renormalization scale for values above 1 GeV [7]. Finally, in their analysis of ε'/ε the authors of Ref. [36] considered B_6 and B_8 as free parameters to be varied around the VSA values $B_6^{(1/2)} = B_8^{(3/2)} = 1$.

We note that our result for $B_6^{(1/2)}$ is in rough agreement with those of the various studies quoted above, whereas the value we obtain for $B_8^{(3/2)}$ lies below the values reported previously. It is desirable to investigate whether this substantial reduction of $\langle Q_8\rangle_2$, which is due to the non-factorizable $1/N_c$ corrections to the leading term in the chiral expansion of Q_8, will be affected by higher order corrections. This point is of great phenomenological interest because a less effective cancellation between the Q_6 and Q_8 operators, in the range obtained in the present analysis, will lead to a large value of ε'/ε in the ball park of $\sim 10^{-3}$. This can be confirmed or disproved by the forthcoming experiments at CERN (NA48), Fermilab (E832) and Frascati (KLOE).

7 Summary

It was recognized, long ago, that the operators Q_6 and Q_8 are of central importance for the determination of the CP parameter ε'/ε. This makes the calculation of their matrix elements imperative as the Wilson coefficients are known to a good degree of accuracy. We carried out this calculation in the $1/N_c$ expansion, where we included terms up to $\mathcal{O}(p^2)$ and $\mathcal{O}(p^0/N_c)$. In doing so we introduced several improvements. First we used the complete pseudoscalar lagrangian relevant to these orders and included effects of the singlet η_0, which we found to be small. At the same time we paid special attention on the definition of the momenta in the chiral loop corrections. To this end, we considered the exchange of a bosonic field between the quark densities whose momentum is taken to be the same at long and short distances. In this approach we set up the identification of the ultraviolet cutoff of the long-distance terms with the QCD renormalization scale. This procedure leads naturally to the classification of the diagrams into factorizable and non-factorizable.

We showed explicitly, to $\mathcal{O}(p^0/N_c)$, that the factorizable scale of the chiral loop corrections is absorbed in the renormalization of the low-energy lagrangian. Thus for the factorizable terms the matching of long- and short-distance contributions is between the running quark masses and quark densities where the matching is exact, i.e., the scale dependence drops out. There remain the non-factorizable terms where we showed explicitly that the dependence on the cutoff, to the order of our calculation, is only logarithmic. Our analysis was carried through using two different techniques. The first one is an explicit calculation of the matrix elements at the particle level which involves a large number of diagrams. The second is the background field method. It leads to operator relations which can be applied also to $K \to 3\pi$ decays. We verified that both techniques give the same results for the quadratic and logarithmic terms. The full finite corrections were calculated at the particle level.

Finally, we determined the numerical values of the matrix elements. We obtained moderate corrections to $\langle Q_6\rangle_0$ and a large decrease of $\langle Q_8\rangle_2$. Each of these matrix elements depends on the renormalization scale, but it is significant to emphasize that their ratio is fairly stable. The numerical results indicate that loop corrections are important and must be included. We note that the terms of $\mathcal{O}(p^0/N_c)$ we calculated here are lowest order corrections to the well established $\mathcal{O}(p^2)$ chiral lagrangian and do not contain any large ambiguity. It remains to be seen whether the results of Tables 1 and 2 will be affected by higher order corrections. This point is important because a cancellation between the gluon and the electroweak penguins in the range obtained in the present analysis will lead to a

large value of $\varepsilon'/\varepsilon \sim 10^{-3}$.

Acknowledgments

We wish to thank Johan Bijnens, Jorge Fatelo and Jean-Marc Gérard for helpful comments. The research of W.B. is supported by Fermi National Accelerator Laboratory, operated by Universities Research Association under contract no. DE-AC02-76CHO3000 with the United States Department of Energy. T.H. and P.S. wish to thank the Deutsche Forschungsgemeinschaft for a fellowship (T.H.) and a scholarship (P.S.) in the Graduate Program for Elementary Particle Physics at the University of Dortmund.

A Bare Parameters

In terms of the basic integrals the full expressions needed for the renormalization procedure read

$$Z_\pi = 1+\frac{8L_5}{f^2}m_\pi^2-\frac{1}{3f^2}\Big(2I_1[m_\pi]+I_1[m_K]\Big)\,, \tag{58}$$

$$Z_K = 1+\frac{8L_5}{f^2}m_K^2-\frac{1}{4f^2}\Big(I_1[m_\pi]+2I_1[m_K]+\cos^2\theta\; I_1[m_\eta]+\sin^2\theta\; I_1[m_{\eta'}]\Big)\,, \tag{59}$$

$$m_\pi^2 = r\hat{m}\bigg[1-\frac{8m_\pi^2}{f^2}(L_5-2L_8)+\frac{1}{6f^2}\Big(3I_1[m_\pi]-a^2I_1[m_\eta]-2b^2I_1[m_{\eta'}]\Big)\bigg]\,, \tag{60}$$

$$\begin{aligned} m_K^2 = {} & r\frac{\hat{m}+m_s}{2}\bigg[1-\frac{8m_K^2}{f^2}(L_5-2L_8) \\ & -\frac{1}{36f^2m_K^2}\Big[I_1[m_\eta]\Big(m_\pi^2(a^2-4b^2)-8m_K^2(a-b)b-m_\eta^2(a+2b)^2\Big) \\ & +2I_1[m_{\eta'}]\Big(2m_K^2a(a+2b)-m_\pi^2(a^2-b^2)-m_{\eta'}^2(a-b)^2\Big)\Big]\bigg]\,, \end{aligned} \tag{61}$$

$$F_\pi = f\left[1+\frac{4L_5}{f^2}m_\pi^2-\frac{1}{2f^2}\Big(2I_1[m_\pi]+I_1[m_K]\Big)\right]\,, \tag{62}$$

$$F_K = f\left[1+\frac{4L_5}{f^2}m_K^2-\frac{3}{8f^2}\Big(I_1[m_\pi]+2I_1[m_K]+\cos^2\theta\; I_1[m_\eta]+\sin^2\theta\; I_1[m_{\eta'}]\Big)\right]\,. \tag{63}$$

a, b and θ are defined in Eqs. (10) and (19), the integral $I_1[m]$ in Eq. (64) of Appendix B. Eqs. (59)–(61) and (63) differ from the corresponding expressions in Ref. [14] on account of the presence of the η_0 state. In the octet limit [$\theta = 0$, $m_\eta^2 = (4m_K^2 - m_\pi^2)/3$] Eqs. (58)–(63) are in agreement with Ref. [14].[8] We note that the η_0 state modifies the logarithmic dependence of the L_8 coefficient on the renormalization scale, whereas it does not affect the corresponding term in L_5.

In the cutoff regularization scheme Eqs. (58)–(63) together with the explicit form of the integral I_1 given in Eq. (67) of Appendix B lead to the formulas listed in Section 4.1, in which the finite terms have been omitted.

In the numerical analysis of the matrix elements dimensional regularization has been used for the factorizable part, as argued at the end of Section 4.2, and the integral I_1 has been calculated in the standard way. The full expressions for the (renormalized) parameters

[8] The comparison is carried out by omitting the L_4 and L_6 terms which are subleading in N_c.

f, L_5 and L_8 have been obtained from Eqs. (60)–(63) by replacing f byF_π (or F_K) in the $\mathcal{O}(p^2)$ and $\mathcal{O}(p^0/N_c)$ terms, as discussed at the end of Section 4.1.

B Basic Integrals

Using algebraic relations the complex structures of the four-dimensional integration can be reduced to three basic components:

$$I_1[m] = \frac{i}{(2\pi)^4}\int d^4q\,\frac{1}{q^2-m^2}\,, \tag{64}$$

$$I_2[m,p] = \frac{i}{(2\pi)^4}\int d^4q\,\frac{1}{(q-p)^2-m^2}\,, \tag{65}$$

$$I_3[m_1,m_2,p] = \frac{i}{(2\pi)^4}\int d^4q\,\frac{1}{(q^2-m_1^2)[(q-p)^2-m_2^2]}\,. \tag{66}$$

Performing a Wick-rotation to Euclidian space-time the ultraviolet cutoff may be implemented through the step-function $\theta(\Lambda_c^2-q_E^2)$. A straightforward calculation then yields

$$I_1[m] = \frac{1}{16\pi^2}\left[\Lambda_c^2 - m^2\log\left(1+\frac{\Lambda_c^2}{m^2}\right)\right]. \tag{67}$$

In order to determine I_2 and I_3 analytically we shift the variable q by the external momentum. Properly taking into account the resulting modification of the upper bound we introduce an angular-dependent argument of the step-function. However, we omit the explicit angular-integration writing the latter function in terms of a Taylor-series:

$$\theta(\Lambda_c^2-q_E'^2+a) = \theta(\Lambda_c^2-q_E'^2) + \sum_{m=0}^{\infty}(-1)^m\frac{d^m\delta(\Lambda_c^2-q_E'^2)}{d(q_E'^2)^m}\frac{a^{m+1}}{(m+1)!}\,. \tag{68}$$

The corresponding solution of the integral I_2 reads

$$\begin{aligned} I_2[m,p] &= \frac{1}{16\pi^2}\left\{\Lambda_c^2 - m^2\log\left(1+\frac{\Lambda_c^2}{m^2}\right) + \frac{p^2\Lambda_c^4}{2(\Lambda_c^2+m^2)^2}\right. \\ &\left. + \frac{p^4\Lambda_c^4m^2}{2(\Lambda_c^2+m^2)^4} - \frac{p^6\Lambda_c^4m^2}{3(\Lambda_c^2+m^2)^6}\left(\Lambda_c^2-\frac{3}{2}m^2\right)\right\} + \mathcal{O}(p^8)\,. \end{aligned} \tag{69}$$

The computation of I_3 requires a Feynman-parametrization:

$$I_3[m_1,m_2,p] = \int_0^1 dx\int\frac{id^4q}{16\pi^2}\left\{(q-xp)^2 - \left[x^2p^2 - x(p^2+m_1^2-m_2^2)+m_1^2\right]\right\}^{-2}. \tag{70}$$

Performing the Wick-rotation and introducing the variable $q_E' = q_E - xp_E$ we obtain

$$I_3[m_1,m_2,p_E] = -\frac{1}{16\pi^2}\int_0^1 dx\int d^4q_E'\frac{1}{\left[q_E'^2+M^2(x)\right]^2}\theta\left[\Lambda_c^2 - q_E'^2 - 2x(q'p)_E - x^2p_E^2\right]\,, \tag{71}$$

with

$$M^2(x) = -x^2 p_E^2 + x(p_E^2 - m_1^2 + m_2^2) + m_1^2 \,. \tag{72}$$

For distinct masses m_1 and m_2 Eq. (71) yields

$$\begin{aligned}
I_3[m_1, m_2, p] \;=\; & \frac{1}{16\pi^2}\Bigg\{ \frac{\sqrt{-w}}{p^2}\Bigg(\arctan\left[\frac{m_1^2 - m_2^2 + p^2}{\sqrt{-w}}\right] + \arctan\left[\frac{m_2^2 - m_1^2 + p^2}{\sqrt{-w}}\right]\Bigg) \\
& + \frac{1}{p^2}(m_2^2 - m_1^2)\log\left(\frac{m_2}{m_1}\right) - 1 + \log\left(\frac{m_1 m_2}{\Lambda_c^2 + m_2^2}\right) + \frac{m_1^2}{m_1^2 - m_2^2}\log\left(\frac{\Lambda_c^2 + m_2^2}{\Lambda_c^2 + m_1^2}\right) \\
& + \frac{p^2 m_2^2}{2(m_1^2 - m_2^2)^2}\left[\frac{1}{(\Lambda_c^2 + m_2^2)^2}(2\Lambda_c^2 m_1^2 + m_1^2 m_2^2 + m_2^4) + \frac{2m_1^2}{m_1^2 - m_2^2}\log\left(\frac{\Lambda_c^2 + m_2^2}{\Lambda_c^2 + m_1^2}\right)\right] \\
& + \frac{p^4 m_2^2}{(m_1^2 - m_2^2)^4}\Bigg[\frac{1}{6(\Lambda_c^2 + m_2^2)^4}\Big(6\Lambda_c^6 m_1^2(m_1^2 + m_2^2) + 3\Lambda_c^4 m_1^2(-m_1^4 + 6m_1^2 m_2^2 + 7m_2^4) \\
& + 2\Lambda_c^2 m_2^2(2m_1^4 m_2^2 + 17 m_1^2 m_2^4 - m_2^6) + m_2^6(m_1^4 + 10 m_1^2 m_2^2 + m_2^4)\Big) \\
& + \frac{m_1^2(m_1^2 + m_2^2)}{(m_1^2 - m_2^2)}\log\left(\frac{\Lambda_c^2 + m_2^2}{\Lambda_c^2 + m_1^2}\right)\Bigg]\Bigg\} + \mathcal{O}(p^6)\,,
\end{aligned} \tag{73}$$

where we defined

$$w = \left(m_1^2 + m_2^2 - p^2\right)^2 - 4m_1^2 m_2^2 \,. \tag{74}$$

As I_3 starts only logarithmically in the cutoff dependence, in Eq. (73) we truncated the series including only terms up to the order p^4.

In the case of equal masses we perform a power series expansion with respect to the parameter $\delta m^2 = m_1^2 - m_2^2$. Then putting δm^2 to zero we find

$$\begin{aligned}
I_3[m_1 = m_2, p] \;=\; & \frac{1}{16\pi^2}\Bigg\{ \frac{2\sqrt{-w}}{p^2}\arctan\left(\frac{p^2}{\sqrt{-w}}\right) - 1 - \frac{m_1^2}{\Lambda_c^2 + m_1^2} + \log\left(\frac{m_1^2}{\Lambda_c^2 + m_1^2}\right) \\
& + p^2\frac{(3\Lambda_c^2 + m_1^2)m_1^2}{6(\Lambda_c^2 + m_1^2)^3} + p^4\frac{(-20\Lambda_c^4 + 5\Lambda_c^2 m_1^2 + m_1^4)m_1^2}{60(\Lambda_c^2 + m_1^2)^5}\Bigg\} + \mathcal{O}(p^6)\,.
\end{aligned} \tag{75}$$

with w being reduced to $w = p^4 - 4p^2 m_1^2$.

Through analytic continuation, Eqs. (73) and (75) provide complex solutions. These appear for $\sqrt{p^2} > m_1 + m_2$. In the process under consideration, the latter relation can only be satisfied for $m_1 = m_2 = m_\pi$, $p = p_K$. Thus our analysis gives the physical threshold condition for $\pi - \pi$ rescattering, the imaginary part of I_3 being attributed to the strong final state interaction phase.

References

[1] W.A. Bardeen, A.J. Buras, and J.-M. Gérard, Nucl. Phys. **B293**, (1987) 787; Phys. Lett. **B192**, (1987) 138; **B211**, (1988) 343.

[2] G. Buchalla, A.J. Buras, and M.K. Harlander, Nucl. Phys. **B337**, (1990) 313.

[3] J.-M. Schwarz *Diploma thesis*, Dortmund 1991; J. Heinrich and J.-M. Schwarz, *Internal Report Univ. of Dortmund* 1992-01; J. Heinrich, E.A. Paschos, J.-M. Schwarz, and Y.L. Wu, Phys. Lett. **B279**, (1992) 140.

[4] E.A. Paschos, in *17th International Symposium on Lepton-Photon Interactions: LP95*, Proceedings, Beijing, China, 1995, edited by Zhi-Peng Zheng and He-Sheng Chen (World Scientific, Singapore, 1996).

[5] A.J. Buras and J.-M. Gérard, Phys. Lett. **B 192**, (1987) 156.

[6] M.K. Gaillard and B.W. Lee, Phys. Rev. Lett. **33**, (1974) 108; G. Altarelli and L. Maiani, Phys. Lett. **B52**, (1974) 351; F.J. Gilman and M.B. Wise, Phys. Rev. **D20**, (1979) 2392; B. Guberina and R.D. Peccei, Nucl. Phys. **B163**, (1980) 289.

[7] A.J. Buras, M. Jamin, M.E. Lautenbacher, and P.H. Weisz, Nucl. Phys. **B400**, (1993) 37, 75; A.J. Buras, M. Jamin, and M.E. Lautenbacher, Nucl. Phys. **B408**, (1993) 209.

[8] M. Ciuchini, E. Franco, G. Martinelli, and L. Reina, Phys. Lett. **B301**, (1993) 263.

[9] M.K. Gaillard and B.W. Lee, Phys. Rev. **D10**, (1974) 897.

[10] A.A. Penin and A.A. Pivoravov, Int. J. Mod. Phys. **A10**, (1995) 4065.

[11] S. Bertolini, J.O. Eeg, and M. Fabbrichesi, Nucl. Phys. **B476**, (1996) 225.

[12] A.A. Bel'kov, G. Bohm, A.V. Lanyov, and A.A. Moshkin, talk presented at the Workshop of the NA48 Collaboration, Dubna, Russia (Feb 1997), Report No. JINR-E2-97-139 (hep-ph/9704354).

[13] J. Bijnens, E. Pallante, and J. Prades, report BERN-98/02 (hep-ph/9801326).

[14] J. Gasser and H. Leutwyler, Nucl. Phys. **B250**, (1985) 465, 517, 539.

[15] G. 't Hooft, Nucl. Phys. **B72**, (1974) 461; Nucl. Phys. **B75**, (1974) 461.

[16] A.J. Buras, in *CP Violation*, (1989) 575, edited by C. Jarlskog (World Scientific, Singapore).

[17] C. Lovelace, Phys. Lett. **B28**, (1968) 264.

[18] W.A. Bardeen, talk presented at the Workshop on Hadronic Matrix Elements and Weak Decays, Ringberg Castle, Germany (April 1988), published in Nucl. Phys. Proc. Suppl. **7A**, (1989) 149.

[19] J. Bijnens, J.-M. Gérard, and G. Klein, Phys. Lett. **B257**, (1991) 191.

[20] J.P. Fatelo and J.-M. Gérard, Phys. Lett. **B347**, (1995) 136.

[21] J. Bijnens and J. Prades, Nucl. Phys. **B444**, (1995) 523.

[22] J.-M. Gérard, Mod. Phys. Lett. **A5**, (1990) 391.

[23] M. Fabbrichesi and E.I. Lashin, Phys. Lett. **B387**, (1996) 609.

[24] S. Bertolini, J.O. Eeg, M. Fabbrichesi, and E.I. Lashin, Nucl. Phys. **B514**, (1998) 93.

[25] W.A. Bardeen (1988, unpublished).

[26] J. Bijnens, G. Ecker, and J. Gasser, contribution to the 2nd DAPHNE *Physics Handbook*, 125 (hep-ph/9411232).

[27] H. Leutwyler, Phys. Lett. **B378**, (1996) 313.

[28] G. Buchalla, A.J. Buras, and M.E. Lautenbacher, Rev. Mod. Phys. **68**, (1996) 1125.

[29] P.H. Soldan, talk presented at the Workshop on K Physics, Orsay, France (May 1996), published in the proceedings (hep-ph/9608281).

[30] G. Kilcup, in *Lattice '90*, Proceedings of the International Symposium, Tallahassee, Florida, edited by V.M. Heller *et al.* [Nucl. Phys. **B (Proc. Suppl.) 20**, (1991) 417].

[31] S. Sharpe, in *Lattice '90*, Proceedings of the International Symposium, Tallahassee, Florida, edited by V.M. Heller *et al.* [Nucl. Phys. **B (Proc. Suppl.) 20**, (1991) 429].

[32] D. Pekurovsky and G. Kilcup, in *Lattice '97*, Proceedings of the International Symposium, Edinburgh, Scotland, edited by C. Davies *et al.* [Nucl. Phys. **B (Proc. Suppl.) 63**, (1998) 293], hep-lat/9709146.

[33] T. Bhattacharya, R. Gupta, and S. Sharpe, Phys. Rev. **D55**, (1997) 4036.

[34] G. Kilcup, R. Gupta, and S. Sharpe, Phys. Rev. **D57**, (1998) 1654.

[35] L. Conti, A. Donini, V. Gimenez, G. Martinelli, M. Talevi, and A. Vladikas, report Edinburgh 97-12 (hep-lat/9711053).

[36] A.J. Buras, M. Jamin, and M.E. Lautenbacher, Phys. Lett. **B389**, (1996) 749.

Figure Captions

Fig. 1 Matching of short- and long-distance contributions.

Fig. 2 Tree plus factorizable loop diagrams for the $K \to \pi\pi$ matrix elements of Q_6 and Q_8; the crossed circles denote the bosonized densities, the black circles the strong interaction vertices. The external lines represent all possible configurations of the kaon and pion fields.

Fig. 3 Same as in Fig. 2, now for the non-factorizable loop diagrams.

Fig. 4 Evolution of the density operator; the black circle, square and triangle denote the kinetic, mass and $U_A(1)$ breaking terms in Eq. (41), the crossed circle the density of Eq. (42). The lines represent the ξ propagators.

Fig. 5 Evolution of the current operator. The crossed circle here denotes the bosonized current.

Fig. 6 Evolution of the kinetic operator (wave function renormalization).

Fig. 7 Evolution of the mass operator (mass renormalization).

Fig. 8 Non-factorizable loop diagrams for the evolution of a density$\times$density operator.

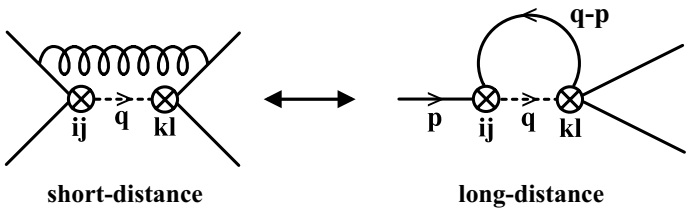

Fig. 1

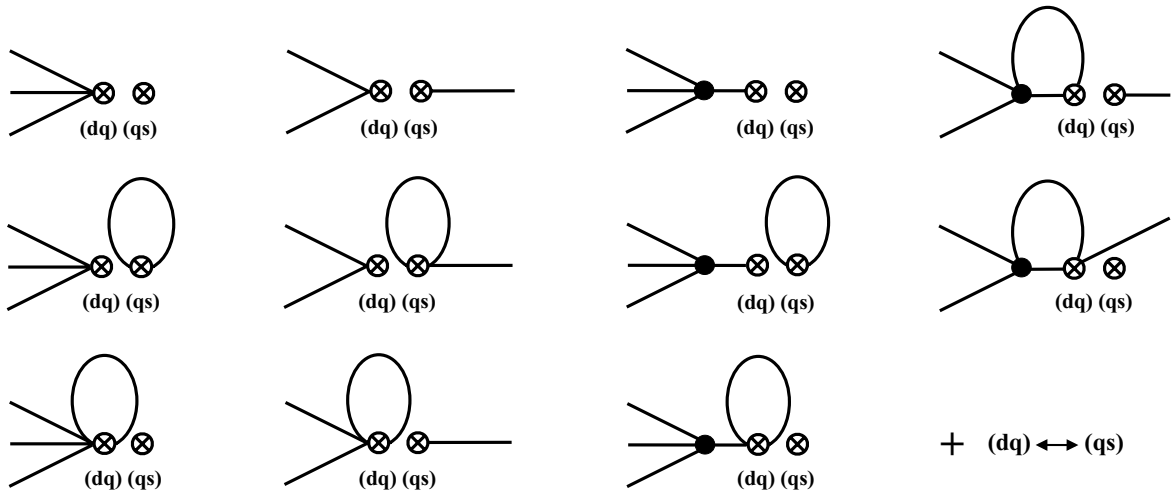

Fig. 2

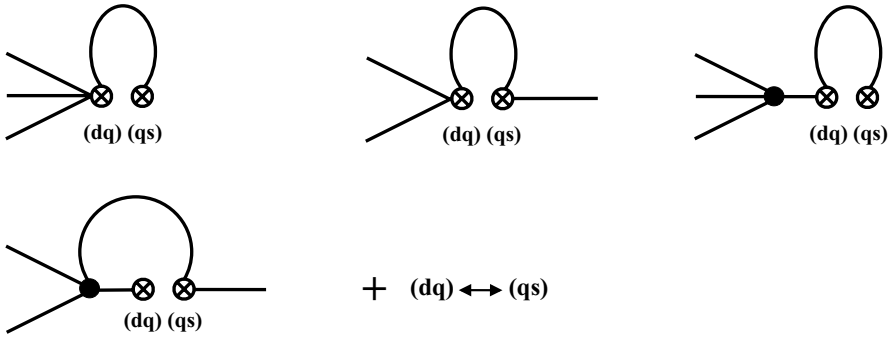

Fig. 3

Fig. 4

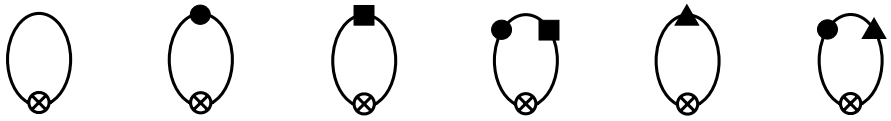

Fig. 5

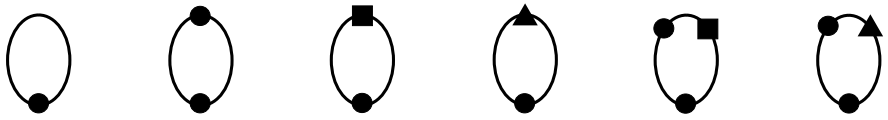

Fig. 6

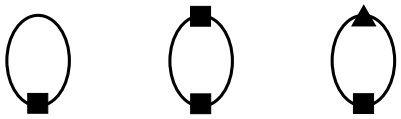

Fig. 7

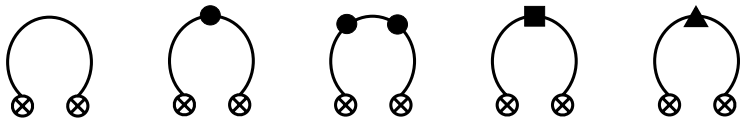

Fig. 8